Evaluating climate model performance in the tropics with retrievals of water isotopic composition from Aura TES

Robert D. Field[1,2], Daehyun Kim[3], Allegra N. LeGrande[1] , John Worden[4], Maxwell Kelley[1,5], Gavin A. Schmidt[1]

1. NASA Goddard Institute for Space Studies, New York, NY, USA
2. Dept. of Applied Physics and Applied Mathematics, Columbia University, New York, NY, USA
3. Department of Atmospheric Sciences, University of Washington, Seattle, WA, USA.
4. Jet Propulsion Laboratory/California Institute of Technology, Pasadena, CA, USA
5. Trinnovim LLC, New York, New York, USA

This article has been accepted for publication and undergone full peer review but has not been through the copyediting, typesetting, pagination and proofreading process which may lead to differences between this version and the Version of Record. Please cite this article as doi: 10.1002/2014GL060572

Abstract

We evaluate the NASA GISS ModelE2 general circulation model over the tropics against water isotope (HDO/H_2O) retrievals from the Aura Tropospheric Emission Spectrometer (TES). Observed isotopic distributions are distinct from other observable quantities and can therefore act as an independent constraint. We perform a small ensemble of simulations with physics perturbations to the cumulus and planetary boundary layer schemes. We examine the degree to which model-data agreement could be used to constrain a select group of internal processes in the model, namely condensate evaporation, entrainment strength, and updraft mass flux. All are difficult to parameterize, but exert strong influence over model performance. We find that the water isotope composition is more sensitive to physics changes than precipitation, temperature or relative humidity in the lower and upper tropical troposphere. Among the processes considered, this is most closely, and fairly exclusively, related to mid-tropospheric entrainment strength. Our study indicates that water isotope observations could provide useful constraints on model parameterizations.

Introduction

Observational and theoretical arguments suggest that satellite retrievals of stable water isotope composition of water vapor are useful for climate model evaluation [Sherwood et al., 2010]. The isotopic composition of water vapor is controlled by the same processes that control water vapor amount, but the observed distribution of isotopic composition is distinct from the amount itself [Worden et al., 2007]. This is due to the fractionation that occurs between the abundant $H_2{}^{16}O$ isotopes (isotopologues) and the rare and heavy $H_2{}^{18}O$ and HDO ($^1H^2H^{16}O$) isotopes during evaporation and condensation. The fractionation physics are simpler than the underlying moist physics; discrepancies between observed and modeled isotopic fields are therefore more likely due to problems in the underlying moist physics. Isotopic measurements therefore have the potential for identifying problems in global climate models that might not be apparent from more conventional measurements.

Isotopic tracers have existed in climate models since the 1980s [e.g. Joussaume et al., 1984; Jouzel et al., 1987], but it is only since the mid 2000s that there have been enough data [e.g. Frankenberg et al., 2009; Worden et al., 2012] for meaningful model evaluation in this sense, in the troposphere at least. Water isotope retrievals from the Tropospheric Emission Spectrometer (TES) on board Aura, among other instruments, have shown promise in evaluating model components related to the timescale of convective instability decay in the NCAR CAM model [Lee et al., 2009], for example, which was identified by Yang et al. [2013] as a free parameter to which CAM precipitation quality was highly sensitive. Risi et al. [2012] used isotopic measurements to identify overly-strong diffusion during vapor transport for a model with a degraded advection scheme as a primary cause of a moist tropospheric bias in the LMDZ model.

In this paper, we examine a small ensemble of perturbed physics experiments with the NASA GISS ModelE2 general circulation model (GCM) for their isotopic response alongside more conventional measurements. The physics perturbations are to the cumulus and planetary boundary layer schemes, done in the context of the normal model development process, where separate but interacting components of the model are being changed simultaneously. We examine the spread in model-observation agreement for different measurements, and determine whether this spread can be related to, and therefore constrain, specific internal processes.

Data and model experiments

The atmosphere-only version of ModelE2 used for the CMIP5 experiments (GISS-E2) was assessed by IPCC AR5 and is our starting point for this study [Schmidt et al., 2014]. We referred to it hereafter as the AR5 version. We also use various modifications on this model with physics perturbations as summarized in Table 1, drawn from the PBL changes described in Yao and Cheng [2012] and convective scheme changes described by Kim et al. [2012]. The model with the full set of physics changes is referred to as the AR5' (AR5-'prime') version.

The isotope physics in the model follows the description in Schmidt et al. [2005], and as discussed in that paper and elsewhere [Bolot et al., 2013], there remains uncertainty in the isotopic physics, particularly for kinetic effects and under cold conditions. Previous ModelE experiments [Schmidt et al., 2005] showed that the isotopic response to uncertainty in the simple supersaturation scheme of Jouzel et al. [1987], for example, is strong in the upper tropical troposphere and stratosphere, but small at lower altitudes. This was also seen in Bolot et al. [2013], where the isotopic response to parameter changes generally became strong only when temperature was well-below freezing. Any attempt to constrain UTLS processes using isotopic retrievals from MIPAS [Steinwager et al., 2007] or ACE [Nassar et al., 2007], for example, would be more sensitive to the uncertainties in isotopic physics. For our purposes these issues are beyond the scope of this paper, but will be considered in future work.

We conduct a set of 18 experiments across a representative set of intermediate configurations, with the AR5 and AR5' as end-members. Each experiment is run for seven years with a one year spin up, with prescribed, interannually-varying sea surface temperatures (SST) starting in 2005 to match the TES period. Precipitation is compared to estimates from the Global Precipitation Climatology

Project [Adler et al., 2003]. Temperature and relative humidity are compared to ERA-Interim reanalysis [Dee et al., 2011]. Isotopic composition is denoted as $\delta D \equiv (R_{sample}/R_{std}-1)X1000$, where R_{sample} is the ratio of heavy to light isotope in the measurement and R_{std} is that of standard mean ocean water. δD is compared to TES over the 500-850 hPa range, where the TES retrievals are most sensitive [Worden et al., 2012]. Model δD are compared to TES δD after estimating instrument-equivalent model fields as described in Field et al. [2012], to account for the effect of thick clouds, for example. Following Worden et al [2012], a -6.3% correction is applied to the retrieved HDO concentrations to account for spectroscopic bias. The in-situ data available for estimating this correction are limited to Hawaii [Worden et al., 2011] and the interior of Alaska [Herman et al., 2014], and as such, it is uncertain. This guides our model-data comparisons, similar to previous work [Yoshimura et al., 2011; Risi et al., 2012]. The analysis is over a narrow tropical domain between 15S and 15N, where, cloud effects notwithstanding, TES δD retrievals tend to be of better quality and where our instrument-equivalent δD model fields are more reliable [Field et al., 2012]. We exclude TOA radiation balance as a hard constraint, and in general avoid identifying certain configurations as better than others.

We examine the degree to which model-data agreement could be used to constrain a select group of sub-grid scale processes in the model. Convective condensate re-evaporation is chosen given its important influence on model performance for ModelE2 [Kim et al., 2012] and other models [e.g. Maloney and Hartmann, 2001; Bacmeister et al., 2006; Hohenegger and Bretherton, 2010; Gueremy, 2011] and also on isotopic composition suggested previously [e.g. Worden et al., 2007; Noone, 2012]. Cumulus entrainment strength is important in influencing the sensitivity of the convective column to environmental humidity [e.g. de Rooy et al., 2013], along with convective condensate re-evaporation [Del Genio et al., 2012; Kim et al., 2012]. These are difficult to parameterize and exert strong influence over model behavior in ModelE2 [Kim et al., 2012] and in GCMs more generally [Knight et al., 2007; Rougier et al., 2009; Sanderson et al., 2011; Yang et al., 2013]. We also consider moist convective air mass flux (MCAMFX) at 850 hPa as a general indicator of convective activity and supply of fresh surface air with high δD to the mid-troposphere.

Re-evaporation strength over a layer is diagnosed from the model as the fraction of total convective condensate in the column that evaporated within the convection scheme. Entrainment strength ε is diagnosed according to the standard definition

$$\varepsilon = \frac{1}{M}\frac{dM}{dz}$$

where M is the mass of the convective plume. These quantities are diagnosed independently of their corresponding physics perturbations to account for them being influenced indirectly by other changes. This allows us to include the structural and parametric changes in Table 1, and provides diagnoses that can be interpreted for other models.

Results

We start by comparing the relative humidity (RH) and δD water vapor responses at over 500-850 hPa for the AR5 and AR5' experiments. $RH_{500\text{-}850}$ estimates from ERA-I have maxima of ~75% over the Maritime Continent, Africa and South America (Figure 1a). ModelE2 AR5 has an RH 3% lower (Figure 1b), and a very similar spatial distribution, with a pattern correlation (r_{pat}, the correlation between the model and data fields at corresponding locations) of 0.87. $RH_{500\text{-}850}$ increases by 7% for AR5' (Figure 1c) relative to AR5 which reduces the model's dry humidity bias relative to ERA over wet regions, but tends to over-moisten the dry subtropics. Overall, there is no significant change in the spatial $RH_{500\text{-}850}$ distribution for AR5' (r_{pat} =0.86). Despite significantly different model physics, both the AR5 and AR5' configurations are in similar agreement to the ERA-I estimates. The precipitation response (Supplemental Figure 1) is marked by a slightly better ITCZ representation, but with an increased wet bias over the "Philippine hotspot" and less precipitation over land, similar to the increased re-evaporation response seen in Bacmeister et al. [2006]. The pattern correlation for AR5 is 0.71 and for AR5' is 0.69. It is hard to judge from the $RH_{500\text{-}850}$ or precipitation if the AR5' configuration is better, despite the large parameterization changes.

TES $\delta D_{500-800}$ has a maximum of -52 ‰ over east Africa and an oceanic maximum in the west Pacific (Figure 2a), different from the broad $RH_{500-850}$ maximum over the Maritime Continent. $\delta D_{500-850}$ is much higher over Africa than South America, which is also different from the distribution of $RH_{500-850}$. The large difference between observed RH and δD patterns suggests immediately that even though the δD is also strongly influenced by the same moist processes, its principal controls are somewhat different and it therefore provides an additional constraint useful for model evaluation.

AR5 $\delta D_{500-850}$ is 15‰ lower than TES across the tropics (Figure 2b) and the pattern agreement is much lower (r_{pat} =0.62) than for RH. This could partly be due to the more sparse horizontal sampling of TES compared to the assimilated RH fields from ERA, but with smoothed model and TES $\delta D_{500-850}$ fields, the AR5 agreement increases only slightly (r_{pat} =0.67). The low δD bias for AR5 is most pronounced over Africa, South America and the oceanic rainbelts. $\delta D_{500-850}$ increases by 19‰ for AR5', leading to a positive but smaller bias relative to TES (Figure 2c). More importantly, the agreement in spatial distribution increases significantly (r_{pat} =0.84), due to a preferential increase in δD over the continents and wet oceanic rainbelts. When we take into account the possible uncertainty in the HDO correction, we conclude that the change in pattern agreement is more important than the reduced bias and is likely robust to uncertainty in the retrieval's HDO correction. We note that similarly strong biases still remain in the METOP/IASI and NDACC/FTIR HDO retrievals, but that the isotopic variability is well captured by the retrievals (Schneider et al., submitted to Atmospheric Measurement Techniques Discussions, 2014). We find also in examining a single level at 500 hPa, where the retrieval sensitivity begins to decrease, that the AR5' δD became too high relative to TES, but that the r_{pat} improvement was the same. The greater robustness of r_{pat} leads us to adopt it as the primary metric in judging model sensitivity to perturbed physics. Using a dimensionless quantity such as r_{pat} also simplifies comparisons of model performance across variables with different scales.

Figure 3 shows the spread in r_{pat} for all 18 experiments across a broader set of observations. Temperature over 500-850 hPa ($T_{500\text{-}850}$) has the least amount of spread, which is unsurprising given that the SST boundary conditions are common to all experiments and will strongly force temperatures in the lower troposphere over the ocean. For precipitation, AR5 and AR5' do not represent 'end-members' in terms of r_{pat} changes; gains made by increasing entrainment tend to be offset by the changes to ATURB (atmospheric turbulence) or increased re-evaporation. The spread in $RH_{500\text{-}850}$ is similar to precipitation, and r_{pat} is slightly lower for AR5' compared to AR5 and several of the intermediate experiments.

The spread in r_{pat} for $\delta D_{500\text{-}850}$ across experiments makes the spread in precipitation and the other tropospheric quantities appear modest. The single biggest gain is from increasing entrainment (MoreEntr), but further gains are made especially through the changes in ATURB. In the upper troposphere, $T_{200\text{-}500}$ agreement decreases slightly for AR5' and remains unchanged for $RH_{200\text{-}500}$, but both experiments lie at the center of spread similar to the lower free troposphere for other intermediate experiments.

At minimum, we interpret the $\delta D_{500\text{-}850}$ r_{pat} spread in Figure 3 to mean that δD is indeed valuable for model evaluation alongside conventional measurements. We make an initial attempt to relate the spreads in r_{pat} to cumulus entrainment strength, cumulus condensate re-evaporation and MCAMFX. To illustrate, Figure 4 shows the spread in $\delta D_{500\text{-}850}$ r_{pat} in terms of the strength of these three processes. These serve a similar purpose to Figure 2 in Yang et al. [2013], which related modeled precipitation quality to variation in nine different convective parameters for a larger perturbed physics ensemble. '*r*' values at the tops of the panels show the linear correlation with 95% confidence intervals. There is no relationship between $\delta D_{500\text{-}850}$ r_{pat} and MCAMFX at 850 hPa; $\delta D_{500\text{-}850}$ agreement in the mid-troposphere could not be related in any simple way to the MCAMFX at a lower height, which we thought would be the case via the supply of vapor with higher δD from the surface. For re-evaporation at 500 hPa, two separate, positively associated regimes exist for experiments with directly and indirectly increasing re-evaporation, but there is no clear linear relationship across all experiments. There is a strong positive linear relationship, however, between $\delta D_{500\text{-}850}$ r_{pat} and the cumulus entrainment strength at 500 hPa. This relationship was fairly smooth across experiments where the cumulus entrainment strength was controlled directly and those where it responded indirectly to other changes, unlike re-evaporation. The mechanism that connects the entrainment strength to δD agreement will require further study. It could be due to both the changes to local convective frequency and depth at each grid point, or to large-scale circulation changes that emerge as a result of the local changes. An increase in the cumulus entrainment strength could, for example, suppress deep convection in relatively dry areas and enhance it in wet areas. This would therefore change the transport of fresh water vapor to high altitudes in those areas. Differential diabatic heating between the relatively dry and wet area would be stronger, which would change large-scale circulations. Further experimentation and diagnosis could also be useful in trying to understand the isotopic 'amount effect', explanations for which vary widely. The effect has been attributed using idealized models to larger raindrops during heavier precipitation [Lee and Fung, 2008], re-evaporation in downdrafts [Risi et al., 2008], the strength and organization of mesoscale convection [Kurita, 2013], and, using a limited domain cloud-resolving model, strength of moisture convergence [Moore et al., 2014].

That $\delta D_{500\text{-}850}$ stands out in terms of its relationship to the cumulus entrainment strength at 500 hPa may be due to the selective heights at which the process variables are examined. When entrainment is examined not just at 500 hPa, the positive relationship between $\delta D_{500\text{-}850}$ r_{pat} and the cumulus entrainment rate is robust through the mid-troposphere (Supplemental Figure 2). Relationships between r_{pat} are also examined for MCAMFX (Supplemental Figure 3) and evaporation (Supplemental Figure 4) at different levels, with no relationship to δD and only weak-moderate negative relationships present for T and RH r_{pat}.

Conclusions

Across a small ensemble of 18 perturbed physics experiments with prescribed SSTs, the distribution of δD in the lower free troposphere is more sensitive to physics changes than that of precipitation, or temperature or relative humidity through the depth of the tropical troposphere. In our case, pattern correlations for δD can be related fairly exclusively to the cumulus entrainment strength through the mid troposphere.

Improvements to a climate model's parameterizations of sub-grid scale physics do not necessarily lead to better agreement with observations, due to previous compensating errors in other parts of the model being exposed with changes elsewhere [Mauritsen et al., 2012]. When making these changes, the more and varied observations used for evaluation, the better, as they can potentially be linked to specific, hard-to-observe processes which underlie model errors [Jakob, 2010]. The new turbulence parameterizations of Yao and Cheng [2012] led to improved simulations of low stratocumulus clouds over the subtropical eastern oceans, and the convection parameterizations used in Kim et al. [2012] led to the appearance of a realistic Madden-Julian Oscillation (Madden and Julian, 1972) in ModelE2. In combination as part of the AR5' changes, however, they only served to substitute one problem with the mean state of tropical precipitation (a double ITCZ) with another (pronounced wet bias over the Philippine hotspot). Despite this tradeoff, the large improvement seen in the lower-tropospheric δD suggests that the AR5' configuration is a better starting point for future model improvement.

The use of water isotope measurements in this way is still in its infancy, and there is still much work to be done to mechanistically understand what controls its distribution. Doing so will make isotopic measurements more useful as an observational constraint for processes such as lower tropospheric mixing, the uncertainty in which is thought to be associated with uncertainty in climate model sensitivity [Sherwood et al., 2014].

Acknowledgements

RF was supported by the NASA Postdoctoral Program and NASA grant NNX13AK46G, and DK by NASA grant NNX13AM18G and the Korea Meteorological Administration Research and Development Program under Grant CATER 2013-3142. Part of this research was carried out at the Jet Propulsion Laboratory, California Institute of Technology, under a contract with the National Aeronautics and Space Administration. Resources supporting this work were provided by the NASA High-End Computing (HEC) Program through the NASA Center for Climate Simulation (NCCS) at Goddard Space Flight Center. All data used in the paper can be obtained from the authors.

References

Adler, R. F., et al. (2003), The version-2 global precipitation climatology project (GPCP) monthly precipitation analysis (1979-present), *Journal of Hydrometeorology*, *4*(6), 1147-1167, doi:10.1175/1525-7541(2003)004<1147:tvgpcp>2.0.co;2.

Bacmeister, J. T., M. J. Suarez, and F. R. Robertson (2006), Rain reevaporation, boundary layer-convection interactions, and Pacific rainfall patterns in an AGCM, *Journal of the Atmospheric Sciences*, *63*(12), 3383-3403, doi:10.1175/jas3791.1.

Bechtold, P., J. P. Chaboureau, A. Beljaars, A. K. Betts, M. Kohler, M. Miller, and J. L. Redelsperger (2004), The simulation of the diurnal cycle of convective precipitation over land in a global model, *Quarterly Journal of the Royal Meteorological Society*, *130*(604), 3119-3137, doi:10.1256/qj.03.103.

Bolot, M., B. Legras, and E. J. Moyer (2013), Modelling and interpreting the isotopic composition of water vapour in convective updrafts, *Atmospheric Chemistry and Physics*, *13*(16), 7903-7935, doi:10.5194/acp-13-7903-2013.

Bony, S., C. Risi, and F. Vimeux (2008), Influence of convective processes on the isotopic composition (delta O-18 and delta D) of precipitation and water vapor in the tropics: 1. Radiative-convective equilibrium and Tropical Ocean-Global Atmosphere-Coupled Ocean-Atmosphere Response Experiment (TOGA-COARE) simulations, *Journal of Geophysical Research-Atmospheres*, *113*(D19), doi:10.1029/2008jd009942.

de Rooy, W. C., P. Bechtold, K. Frohlich, C. Hohenegger, H. Jonker, D. Mironov, A. P. Siebesma, J. Teixeira, and J. I. Yano (2013), Entrainment and detrainment in cumulus convection: an overview, *Quarterly Journal of the Royal Meteorological Society*, *139*(670), 1-19, doi:10.1002/qj.1959.

Dee, D. P., et al. (2011), The ERA-Interim reanalysis: configuration and performance of the data assimilation system, *Quarterly Journal of the Royal Meteorological Society*, *137*(656), 553-597, doi:10.1002/qj.828.

Del Genio, A. D., Y. H. Chen, D. Kim, and M. S. Yao (2012), The MJO Transition from Shallow to Deep Convection in CloudSat/CALIPSO Data and GISS GCM Simulations, *Journal of Climate*, *25*(11), 3755-3770, doi:10.1175/jcli-d-11-00384.1.

Field, R. D., C. Risi, G. A. Schmidt, J. Worden, A. Voulgarakis, A. N. LeGrande, A. H. Sobel, and R. J. Healy (2012), A Tropospheric Emission Spectrometer HDO/H2O retrieval simulator for climate models, *Atmospheric Chemistry and Physics*, *12*(21), 10485-10504, doi:10.5194/acp-12-10485-2012.

Frankenberg, C., et al. (2009), Dynamic Processes Governing Lower-Tropospheric HDO/H2O Ratios as Observed from Space and Ground, *Science*, *325*(5946), 1374-1377, doi:10.1126/science.1173791.

Gueremy, J. F. (2011), A continuous buoyancy based convection scheme: one- and three-dimensional validation, *Tellus Series a-Dynamic Meteorology and Oceanography*, *63*(4), 687-706, doi:10.1111/j.1600-0870.2011.00521.x.

Herman, R. L., J. E. Cherry, J. Young, J. M. Welker, D. Noone, S. S. Kulawik, and J. Worden (2014), Aircraft validation of the Aura Tropospheric Emission Spectrometer retrievals of HDO and H_2O, *Atmospheric Measurement Techniques Discussions*, *7*, 3801-3833, doi:10.5194/amtd-7-3801-2014.

Hohenegger, C., and C. S. Bretherton (2011), Simulating deep convection with a shallow convection scheme, *Atmospheric Chemistry and Physics*, *11*(20), 10389-10406, doi:10.5194/acp-11-10389-2011.

Holtslag, A. A. M., and B. A. Boville (1993), Local versus nonlocal boundary-layer diffusion in a global climate model, *Journal of Climate*, *6*(10), 1825-1842, doi:10.1175/1520-0442(1993)006<1825:lvnbld>2.0.co;2.

Holtslag, A. A. M., and C. H. Moeng (1991), Eddy diffusivity and countergradient transport in the convective atmospheric boundary layer, *Journal of the Atmospheric Sciences*, *48*(14), 1690-1698, doi:10.1175/1520-0469(1991)048<1690:edacti>2.0.co;2.

Jakob, C. (2010), Accelerating progress in global atmospheric model development through improved parameterizations: challenges, opportunities and strategies, *Bulletin of the American Meteorological Society*, *91*(7), 869-+, doi:10.1175/2009bams2898.1.

Joussaume, S., R. Sadourny, and J. Jouzel (1984), A general-circulation model of water isotope cycles in the atmosphere, *Nature*, *311*(5981), 24-29, doi:10.1038/311024a0.

Jouzel, J., G. L. Russell, R. J. Suozzo, R. D. Koster, J. W. C. White, and W. S. Broecker (1987), Simulations of HDO and H_2O^{18} atmospheric cylces using the NASA GISS General Circulation Model - The seasonal cycle for present day conditions, *Journal of Geophysical Research-Atmospheres*, *92*(D12), 14739-14760, doi:10.1029/JD092iD12p14739.

Kim, D., A. D. Del Genio, and M. S. Yao (2013), Moist convection scheme in Model E2*Rep.*, arXiv:1312.7496 pp.

Kim, D., A. H. Sobel, A. D. Del Genio, Y. H. Chen, S. J. Camargo, M. S. Yao, M. Kelley, and L. Nazarenko (2012), The Tropical Subseasonal Variability Simulated in the NASA GISS General Circulation Model, *Journal of Climate*, *25*(13), 4641-4659, doi:10.1175/jcli-d-11-00447.1.

Knight, C. G., et al. (2007), Association of parameter, software, and hardware variation with large-scale behavior across 57,,000 climate models, *Proceedings of the National Academy of Sciences of the United States of America*, *104*(30), 12259-12264, doi:10.1073/pnas.0608144104.

Kurita, N. (2013), Water isotopic variability in response to mesoscale convective system over the tropical ocean, *Journal of Geophysical Research-Atmospheres*, *118*(18), 10376-10390, doi:10.1002/jgrd.50754.

Lee, J.-E., and I. Fung (2008), "Amount effect" of water isotopes and quantitative analysis of post-condensation processes, *Hydrological Processes*, *22*(1), 1-8, doi:10.1002/hyp.6637.

Lee, J. E., R. Pierrehumbert, A. Swann, and B. R. Lintner (2009), Sensitivity of stable water isotopic values to convective parameterization schemes, *Geophysical Research Letters*, *36*, 5, doi:10.1029/2009gl040880.

Madden, R. A., and P. R. Julian (1972), DESCRIPTION OF GLOBAL-SCALE CIRCULATION CELLS IN TROPICS WITH A 40-50 DAY PERIOD, *Journal of the Atmospheric Sciences*, *29*(6), 1109-&, doi:10.1175/1520-0469(1972)029<1109:dogscc>2.0.co;2.

Maloney, E. D., and D. L. Hartmann (2001), The sensitivity of intraseasonal variability in the NCAR CCM3 to changes in convective parameterization, *Journal of Climate*, *14*(9), 2015-2034, doi:10.1175/1520-0442(2001)014<2015:tsoivi>2.0.co;2.

Mauritsen, T., et al. (2012), Tuning the climate of a global model, *Journal of Advances in*

Modeling Earth Systems, *4*, 18, doi:10.1029/2012ms000154.

Nakanishi, M. (2001), Improvement of the Mellor-Yamada turbulence closure model based on large-eddy simulation data, *Boundary-Layer Meteorology*, *99*(3), 349-378, doi:10.1023/a:1018915827400.

Nassar, R., P. F. Bernath, C. D. Boone, A. Gettelman, S. D. McLeod, and C. P. Rinsland (2007), Variability in HDO/H2O abundance ratios in the tropical tropopause layer, *Journal of Geophysical Research-Atmospheres*, *112*(D21), doi:10.1029/2007jd008417.

Noone, D. (2012), Pairing Measurements of the Water Vapor Isotope Ratio with Humidity to Deduce Atmospheric Moistening and Dehydration in the Tropical Midtroposphere, *Journal of Climate*, *25*(13), 4476-4494, doi:10.1175/jcli-d-11-00582.1.

Risi, C., S. Bony, and F. Vimeux (2008), Influence of convective processes on the isotopic composition (delta O-18 and delta D) of precipitation and water vapor in the tropics: 2. Physical interpretation of the amount effect, *Journal of Geophysical Research-Atmospheres*, *113*(D19), doi:10.1029/2008jd009943.

Risi, C., et al. (2012), Process-evaluation of tropospheric humidity simulated by general circulation models using water vapor isotopic observations: 2. Using isotopic diagnostics to understand the mid and upper tropospheric moist bias in the tropics and subtropics, *Journal of Geophysical Research-Atmospheres*, *117*, 25, doi:10.1029/2011jd016623.

Rougier, J., D. M. H. Sexton, J. M. Murphy, and D. Stainforth (2009), Analyzing the Climate Sensitivity of the HadSM3 Climate Model Using Ensembles from Different but Related Experiments, *Journal of Climate*, *22*(13), 3540-3557, doi:10.1175/2008jcli2533.1.

Sanderson, B. M. (2011), A Multimodel Study of Parametric Uncertainty in Predictions of Climate Response to Rising Greenhouse Gas Concentrations, *Journal of Climate*, *24*(5), 1362-1377, doi:10.1175/2010jcli3498.1.

Schmidt, G. A., et al. (2014), Configuration and assessment of the GISS ModelE2 contributions to the CMIP5 archive, *J. Adv. Model. Earth Syst*, *6*, 141-184, doi:10.1002/2013MS000265.

Sherwood, S. C., S. Bony, and J. L. Dufresne (2014), Spread in model climate sensitivity traced to atmospheric convective mixing, *Nature*, *505*(7481), 37-+, doi:10.1038/nature12829.

Sherwood, S. C., R. Roca, T. M. Weckwerth, and N. G. Andronova (2010), Tropospheric water vapor, convection and climate, *Reviews of Geophysics*, *48*, 29, doi:10.1029/2009rg000301.

Steinwagner, J., M. Milz, T. von Clarmann, N. Glatthor, U. Grabowski, M. Hoepfner, G. P. Stiller, and T. Roeckmann (2007), HDO measurements with MIPAS, *Atmospheric Chemistry and Physics*, *7*(10), 2601-2615.

Van Wagner, C. E. (1987), Development and structure of the Canadian Forest Fire Weather Index System*Rep.*, 37 pp, Canadian Forest Service, Ottawa, Canada.

Worden, J., S. Kulawik, C. Frankenberg, V. Payne, K. Bowman, K. Cady-Peirara, K. Wecht, J. E. Lee, and D. Noone (2012), Profiles of CH4, HDO, H2O, and N2O with improved lower tropospheric vertical resolution from Aura TES radiances, *Atmospheric Measurement Techniques*, *5*(2), 397-411, doi:10.5194/amt-5-397-2012.

Worden, J., D. Noone, K. Bowman, and S. Tropospheric Emission (2007), Importance of rain evaporation and continental convection in the tropical water cycle, *Nature*, *445*(7127), 528-532, doi:10.1038/nature05508.

Worden, J., D. Noone, J. Galewsky, A. Bailey, K. Bowman, D. Brown, J. Hurley, S. Kulawik, J. Lee, and M. Strong (2011), Estimate of bias in Aura TES HDO/H2O profiles from comparison of TES and in situ HDO/H2O measurements at the Mauna Loa observatory, *Atmospheric Chemistry and Physics*, *11*(9), 4491-4503, doi:10.5194/acp-11-4491-2011.

Yang, B., et al. (2013), Uncertainty quantification and parameter tuning in the CAM5 Zhang-McFarlane convection scheme and impact of improved convection on the global circulation and climate, *Journal of Geophysical Research-Atmospheres*, *118*(2), 395-415, doi:10.1029/2012jd018213.

Yao, M. S., and Y. Cheng (2012), Cloud Simulations in Response to Turbulence Parameterizations in the GISS Model E GCM, *Journal of Climate*, *25*(14), 4963-4974, doi:10.1175/jcli-d-11-00399.1.

Yoshimura, K., C. Frankenberg, J. Lee, M. Kanamitsu, J. Worden, and T. Rockmann (2011), Comparison of an isotopic atmospheric general circulation model with new quasi-global satellite measurements of water vapor isotopologues, *Journal of Geophysical Research-Atmospheres*, *116*, 15, doi:10.1029/2011jd016035.

Table 1. Changes to convection and turbulence in ModelE2. The AR5 version of the model is described in Schmidt et al. [2014] and the convection scheme in Kim et al. [2013]. The entrainment and re-evaporation changes are discussed in detail in Kim et al. [2012] and the turbulence-related changes in Yao and Cheng [2012].

Parameter	Description	AR5	AR5’
ThetaV	Plume buoyancy threshold for downdraft initiation	θ_v includes water vapor	θ_v includes water vapor and condensate
NewCldBaseEntrLmt	Entrainment mass flux limit	Entrained mass limited to that of plume base layer	Entrained mass limited to that of whole plume
Plume1Entr0.4	Entrainment coefficient for less diluted plume	0.3	0.4
RevpAboveCldBase	Updraft re-evaporation vertical extent	Below cloud only	Entire depth of plume
LessDDraftRevp	Downdraft re-evaporation limit	All condensate allowed to re-evaporate	50% of condensate allowed to re-evaporate
ATURB	Vertical turbulent flux	Diffusive and counter-gradient terms from *Holtslag and Moeng* [1991]	Diffusive and counter-gradient terms from *Holtslag and Boville* [1993]
	Turbulent length scale	*Holtslag and Boville* [1993]	*Holtslag and Boville* [1993] above PBL, *Nakanishi* [2001] within PBL including buoyancy length scale dependent on TKE

PBL height diagnosis	Turbulent kinetic energy profile	Bulk Richardson number criterion from *Holtslag and Boville* [1993]

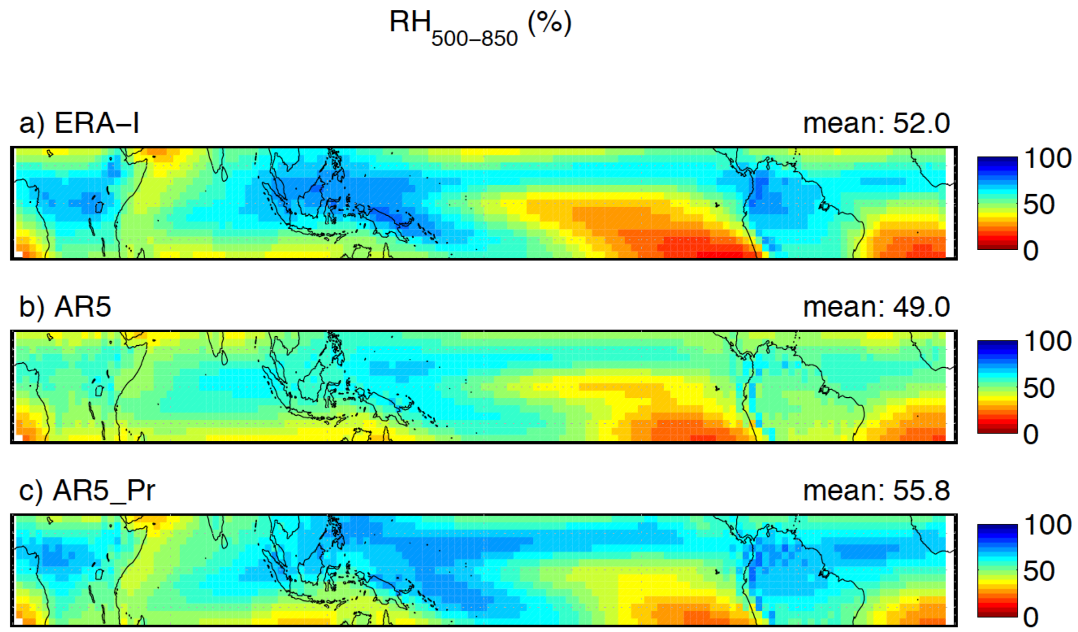

Figure 1. Annual mean RH averaged over 500-850 hPa during 2005-2011 for a) ERA-I b) AR5 c) AR5'.

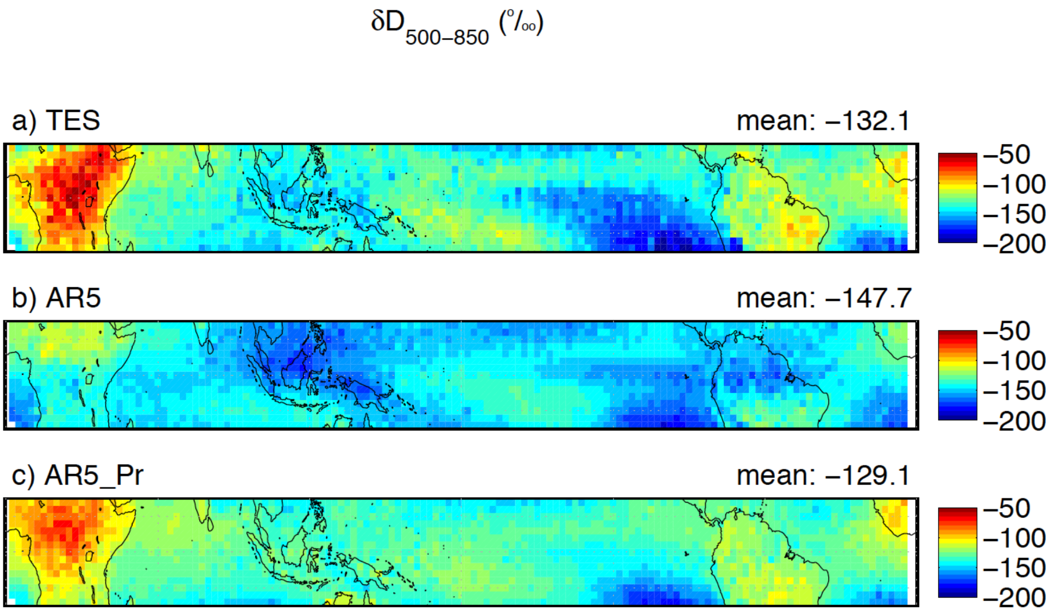

Figure 2. Annual mean δD over 500-850 hPa during 2005-2011 for a) TES b) AR5 c) AR5'.

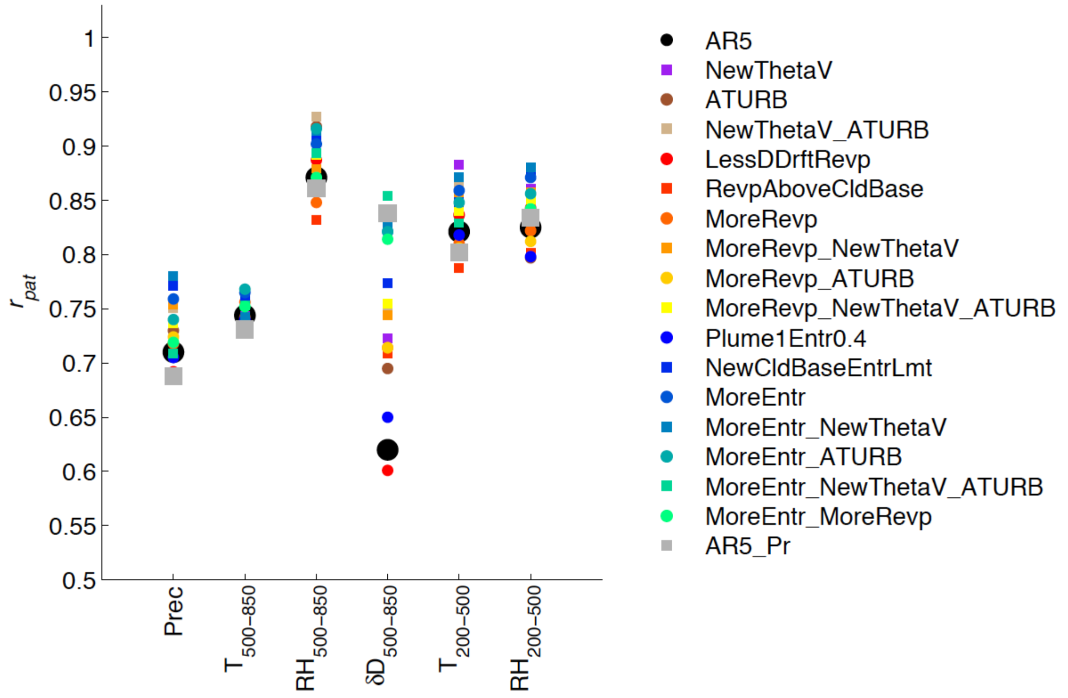

Figure 3. Pattern correlation between model and observations across 18 experiments. Observation types are GPCP precipitation, ERA-Interim temperature and RH averaged over 500-850 hPa and 200-500 hPa, and TES δD averaged over 500-850 hPa.

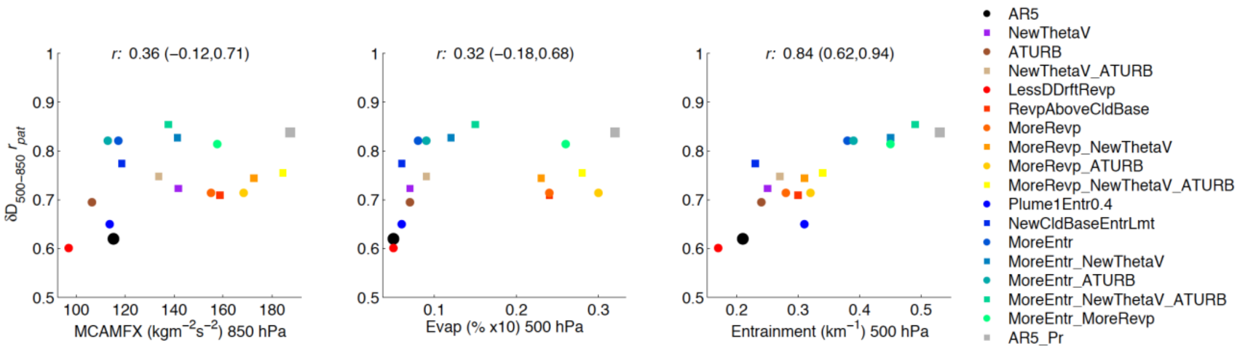

Figure 4. δD$_{500}$ pattern correlation (r_{pat}) between mean annual observations and model fields for 18 experiments as a function of a) moist convective air mass flux (MCAMFX) at 850 hPa b) re-evaporation at 500 hPa, c) entrainment at 500 hPa. 'r' values at the top of each plot (with 95% confidence intervals) are the strength of the linear relationship between the r_{pat} and the process variable.